Technical Note

Vibration Analysis of Axially Functionally Graded Non-Prismatic Euler–Bernoulli Beams Using the Finite Difference Method

Valentin Fogang

Civil Engineer, C/o BUNS Sarl, P.O Box 1130, Yaounde, Cameroon; valentin.fogang@bunscameroun.com

ORCID iD

Abstract: This paper presents an approach to the vibration analysis of axially functionally graded (AFG) non-prismatic Euler–Bernoulli beams using the finite difference method (FDM). The characteristics (cross-sectional area, moment of inertia, elastic moduli, and mass density) of AFG beams vary along the longitudinal axis. The FDM is an approximate method for solving problems described with differential or partial differential equations. It does not involve solving differential equations; equations are formulated with values at selected points of the structure. The model developed in this paper consists of formulating differential or partial differential equations with finite differences and introducing new points (additional or imaginary points) at boundaries and positions of discontinuity (concentrated loads or moments, supports, hinges, springs, and brutal change of stiffness). The introduction of additional points allows satisfying boundary and continuity conditions. Vibration analysis of AFG non-prismatic Euler–Bernoulli beams was conducted with this model, and natural frequencies were determined. Finally, the direct time integration method (DTIM) was presented. The FDM-based DTIM enabled the analysis of forced vibration of AFG non-prismatic Euler–Bernoulli beams, considering the damping. The efforts and displacements could be determined at any time.

Keywords: Axially functionally graded non-prismatic Euler–Bernoulli beam; finite difference method; additional points; vibration analysis; direct time integration method

1.   Introduction

This paper describes the application of Fogang's model [1] based on the finite difference method (FDM), used for the homogeneous Euler–Bernoulli beam, to the vibration analysis of axially functionally graded (AFG) non-prismatic Euler–Bernoulli beam. Various studies have focused on the vibration analysis of AFG Euler–Bernoulli beams. Chen [2] investigated the bending behavior of a non-uniform AFG Euler–Bernoulli beam based on the Chebyshev collocation method; the Chebyshev differentiation matrices were used to reduce the ordinary differential equations into a set of algebraic equations to form the eigenvalue problem associated with the free vibration. Soltani et al. [3] applied the FDM to evaluate natural frequencies of non-prismatic beams with different boundary conditions and resting on variable one- or two-parameter elastic foundations. Torabi et al. [4] presented an exact closed-form solution for free vibration analysis of Euler–Bernoulli conical and tapered beams carrying any desired number of attached masses; the

concentrated masses were modeled by Dirac's delta functions. Liu et al. [5] developed a model for the free transverse vibration of AFG tapered Euler–Bernoulli beam through the spline finite point method; the beam was discretized with a set of uniformly scattered spline nodes along the beam axis, and the displacement field was approximated by the particularly constructed cubic B-spline interpolation functions. Kukla et al. [6] proposed an approach to free vibration analysis of functionally graded beams by approximating the beam by an equivalent beam with piece-wise exponentially varying material and geometrical properties. Cao et al. [7] studied the free vibration of AFG beam using analytical method based on the asymptotic perturbation method and Meijer-Function, respectively.

Classical analysis of the Euler–Bernoulli beam involves solving the governing equations (i.e., statics, dynamics, and material) that are expressed via means of differential equations, considering boundary and continuity conditions. However, solving differential equations may be difficult in the presence of an axial force (or external distributed axial forces), an elastic Winkler foundation, a Pasternak foundation, non-prismatic cross section, non-homogeneous material, or damping (by vibration analysis). In traditional analysis using the FDM, points outside the beam are not considered. The boundary conditions are applied at the beam's ends, not the governing equations. The non-application of governing equations at the beam's ends leads to inaccurate results, making the FDM less useful compared with other numerical methods, such as the finite element method. This paper presented a model based on the FDM. This model consisted of formulating differential equations (statics, dynamics, and material relation) with finite differences and introducing new points (additional or imaginary points) at boundaries and at positions of discontinuity (concentrated loads or moments, supports, hinges, springs, and brutal change of stiffness). The introduction of additional points allowed us to satisfy boundary and continuity conditions. Vibration analysis of structures was conducted using the model.

2.   Materials and methods

2.1   Free vibration analysis

2.1.1   Governing equations of the free vibration

The focus here is to determine the eigenfrequencies of the beam. A second-order analysis is conducted; and the first-order analysis can easily be deduced. The sign convention adopted for loads, bending moments, transverse forces, and displacements is illustrated in Figure 1.
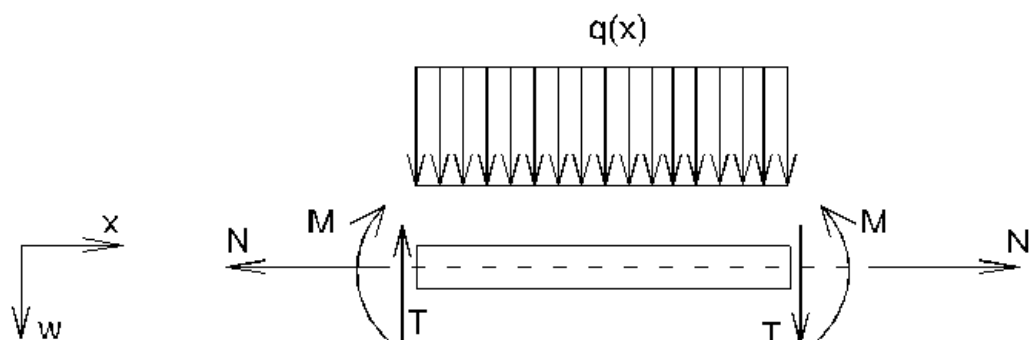
Figure 1.   Sign convention for loads, bending moments, transverse forces, and displacements.

Specifically, M(x) is the bending moment in the section, T(x) is the transverse force, N(x) is the axial force (positive in tension), w(x) is the deflection, and q(x) is the distributed load in the positive downward direction.

Assuming a harmonic vibration, the equations of dynamic equilibrium on an infinitesimal beam element are as follows:

$$\frac{dT(x)}{dx} - k(x)w(x) + \omega^2 \rho(x)A(x)w(x) = 0 \tag{1a}$$

$$\frac{dM(x)}{dx} + N(x)\frac{dw(x)}{dx} - T(x) = 0 \tag{1b}$$

where ρ(x) is the beam's mass per unit volume, A(x) is the cross-sectional area, k(x) is the stiffness of the elastic Winkler foundation, and ω is the circular frequency of the beam. The transverse force T(x) is related to the shear force V(x), as follows:

$$T(x) = V(x) + N(x)\frac{dw(x)}{dx} \cdot \tag{2}$$

Let us consider an external distributed axial load n(x) positive along the + x axis

$$n(x) = -\frac{dN(x)}{dx} \cdot \tag{3}$$

Substituting Equations (2) and (3) into Equations (1a-b) yields

$$\frac{dV(x)}{dx} + N(x)\frac{d^2w(x)}{dx^2} - n(x)\frac{dw(x)}{dx} - k(x)w(x) + \omega^2 \rho(x)A(x)w(x) = 0 \tag{4a}$$

$$\frac{dM(x)}{dx} - V(x) = 0 \cdot \tag{4b}$$

The bending moment, the rotation of the cross section φ(x) (positive in clockwise), and the deflection are related together as follows:

$$M(x) = -E(x)I(x)\frac{d\varphi(x)}{dx} \quad \text{(5a)} \qquad \varphi(x) = \frac{dw(x)}{dx} \quad \text{(5b)}$$

where at a position x, E(x) and I(x) denote the elastic modulus and the moment of inertia, respectively. Combining Equations (4a-b) and (5a-b) yields

$$\frac{d^2M(x)}{dx^2} + N(x)\frac{d^2w(x)}{dx^2} - n(x)\frac{dw(x)}{dx} - k(x)w(x) + \omega^2 \rho(x)A(x)w(x) = 0 \tag{6a}$$

$$M(x) + E(x)I(x)\frac{d^2w(x)}{dx^2} = 0 \tag{6b}$$

Substituting Equation (6b) into (6a) yields

$$-\frac{d^2}{dx^2}\left[E(x)I(x)\frac{d^2w(x)}{dx^2}\right]+N(x)\frac{d^2w(x)}{dx^2}-n(x)\frac{dw(x)}{dx}-k(x)w(x)+\omega^2\rho(x)A(x)w(x)=0\,.$$

(7)

After some manipulations, Equation (7) yields

$$E(x)I(x)\frac{d^4w(x)}{dx^4}+2\frac{d\left[E(x)I(x)\right]}{dx}\frac{d^3w(x)}{dx^3}+\left[\frac{d^2\left[E(x)I(x)\right]}{dx^2}-N(x)\right]\frac{d^2w(x)}{dx^2}$$

$$+n(x)\frac{dw(x)}{dx}+\left[k(x)-\omega^2\rho(x)A(x)\right]w(x)=0\,.$$

(8)

Hence, an M−W FDM approximation (Equations (6a-b)) and a W FDM approximation (Equation (8)) can be considered.

2.1.2 Fundamentals of the FDM

Let us consider a segment k of the beam having equidistant grid points with spacing h_k.

Equations (6a-b) have a second-order derivative; consequently, the deflection and bending moment curves w(x) and M(x), respectively, are approximated around the point of interest i as second-degree polynomials.

Thus, a three-point stencil is used to write finite difference approximations to derivatives at grid points. The derivatives (S(x) representing w(x) or φ(x)) at **i** are expressed with deflection values at points i-1, i, and i+1.

$$\frac{d^2S(x)}{dx^2}\bigg|_i=\frac{S_{i-1}-2S_i+S_{i+1}}{h_k^2}\quad(9a)\qquad\qquad\frac{dS(x)}{dx}\bigg|_i=\frac{-S_{i-1}+S_{i+1}}{2h_k}\quad(9b)$$

Equation (8) has a fourth-order derivative, and the deflection curve is consequently approximated around the point of interest i as a fourth-degree polynomial. Thus, a five-point stencil is used to write finite difference approximations to derivatives at grid points. The derivatives at **i** are expressed with deflection values at points i-2, i-1, i, i+1, and i+2.

$$\frac{d^4w}{dx^4}\bigg|_i=\frac{w_{i-2}-4w_{i-1}+6w_i-4w_{i+1}+w_{i+2}}{h_k^4}$$

(10a)

$$\frac{d^3w}{dx^3}\bigg|_i=\frac{-w_{i-2}+2w_{i-1}-2w_{i+1}+w_{i+2}}{2h_k^3}$$

(10b)

$$\frac{d^2w}{dx^2}\bigg|_i=\frac{-w_{i-2}+16w_{i-1}-30w_i+16w_{i+1}-w_{i+2}}{12h_k^2}$$

(10c)

$$\frac{dw}{dx}\bigg|_i=\frac{w_{i-2}-8w_{i-1}+8w_{i+1}-w_{i+2}}{12h_k}$$

(10d)

2.1.3 FDM Formulation of equations and efforts

2.1.3.1 W FDM approximation

Since the characteristics of the beam vary throughout the longitudinal axis, reference values are defined. The reference values of the beam's mass per unit volume, the cross-sectional area, the moment of inertia, and the elastic modulus are denoted by ρ_r, A_r, I_r, and E_r, respectively. At a position x the beam's mass per unit volume, the cross-sectional area, the moment of inertia, the elastic modulus, and the shear modulus are related to the reference values as follows:

$$E(x) = \beta_E(x) \times E_r \qquad (11a) \qquad\qquad A(x) = \beta_A(x) \times A_r \qquad (11c)$$

$$\rho(x) = \beta_\rho(x) \times \rho_r \qquad (11b) \qquad\qquad I(x) = \beta_I(x) \times I_r \qquad (11d)$$

The reference length is denoted by l_r. We set

$$h_k = \beta_{lk} l_r \qquad (12a) \qquad\qquad W(x) = E_r I_r \times w(x) \qquad (12b)$$

The parameters $\beta'_{EI}(x)$ and $\beta''_{EI}(x)$ are related to the first and second derivative of $\beta_E(x)\beta_I(x)$ with respect to x, respectively, as follows:

$$\beta'_{EI}(x) = h_k \frac{d\left[\beta_E(x)\beta_I(x)\right]}{dx} \qquad (13a) \qquad\qquad \beta''_{EI}(x) = h_k^2 \frac{d^2\left[\beta_E(x)\beta_I(x)\right]}{dx^2} \qquad (13b)$$

The vibration frequency ω is defined as follows:

$$\omega = \lambda \times \sqrt{\frac{E_r I_r}{\rho_r A_r l_r^4}} \qquad (14)$$

Substituting Equations (10a-d), (11a-d), (12a-b), (13a-b), and (14) into Equation (8) yields the FDM formulation of the governing equation as follows:

$$\left[\beta_{Ei}\beta_{Ii} - \beta'_{EIi} - \frac{\beta''_{EIi}}{12} + \frac{N_i h_k^2}{12 E_r I_r} + \frac{n_i h_k^3}{12 E_r I_r}\right]W_{i-2} + \left[-4\beta_{Ei}\beta_{Ii} + 2\beta'_{EIi} + \frac{4\beta''_{EIi}}{3} - \frac{4N_i h_k^2}{3E_r I_r} - \frac{2n_i h_k^3}{3E_r I_r}\right]W_{i-1}$$

$$\left[6\beta_{Ei}\beta_{Ii} - \frac{5\beta''_{EIi}}{2} + \frac{5N_i h_k^2}{2E_r I_r} + \frac{k_i h_k^4}{E_r I_r} - \beta_{lk}^4 \beta_{\rho i}\beta_{Ai}\lambda^2\right]W_i + \left[-4\beta_{Ei}\beta_{Ii} - 2\beta'_{EIi} + \frac{4\beta''_{EIi}}{3} - \frac{4N_i h_k^2}{3E_r I_r} + \frac{2n_i h_k^3}{3E_r I_r}\right]W_{i+1}$$

$$+\left[\beta_{Ei}\beta_{Ii} + \beta'_{EIi} - \frac{\beta''_{EIi}}{12} + \frac{N_i h_k^2}{12 E_r I_r} - \frac{n_i h_k^3}{12 E_r I_r}\right]W_{i-2} = 0 \qquad\qquad (15)$$

The bending moment, the shear force, and the rotation of the cross section are calculated using Equations (6b), (10c), (11a), (11d), and (12b), Equations (4b), (6b), (10b-c), (11a), (11d), (12b), and (13a), and Equations (5b), (10d), and (12b) as follows:

$$M_i = \beta_{Ei}\beta_{Ii}\frac{W_{i-2}-16W_{i-1}+30W_i-16W_{i+1}+W_{i+2}}{12h_k^2} \tag{16a}$$

$$V_i = \beta_{Eli}'\frac{W_{i-2}-16W_{i-1}+30W_i-16W_{i+1}+W_{i+2}}{12h_k^3} + \beta_{Ei}\beta_{Ii}\frac{W_{i-2}-2W_{i-1}+2W_{i+1}-W_{i+2}}{2h_k^3} \tag{16b}$$

$$E_rI_r\varphi_i = \frac{W_{i-2}-8W_{i-1}+8W_{i+1}-W_{i+2}}{12h_k} \tag{16c}$$

Combining Equations (2), (10d), (12b), and (16b) yields the transverse force as follows:

$$T_i = V_i + \frac{N_ih_k^2}{E_rI_r}\frac{W_{i-2}-8W_{i-1}+8W_{i+1}-W_{i+2}}{12h_k^3} \tag{17}$$

For the special case of a beam without an axial force or a Winkler foundation, Equation (15) becomes

$$\left[\beta_{Ei}\beta_{Ii}-\beta_{Eli}'-\frac{\beta_{Eli}''}{12}\right]W_{i-2}+\left[-4\beta_{Ei}\beta_{Ii}+2\beta_{Eli}'+\frac{4\beta_{Eli}''}{3}\right]W_{i-1} \tag{18}$$

$$\left[6\beta_{Ei}\beta_{Ii}-\frac{5\beta_{Eli}''}{2}-\beta_{lk}^4\beta_{\rho i}\beta_{Ai}\lambda^2\right]W_i+\left[-4\beta_{Ei}\beta_{Ii}-2\beta_{Eli}'+\frac{4\beta_{Eli}''}{3}\right]W_{i+1}+\left[\beta_{Ei}\beta_{Ii}+\beta_{Eli}'-\frac{\beta_{Eli}''}{12}\right]W_{i-2}=0$$

2.1.3.2 M−W FDM approximation

Substituting Equations (9a-b), (11a-d), (12a-b), and (14) into Equations (6a-b) yields the FDM formulation of the governing equations as follows:

$$h_k^2M_{i-1}-2h_k^2M_i+h_k^2M_{i+1}+\left(\frac{N_ih_k^2}{E_rI_r}+\frac{n_ih_k^3}{2E_rI_r}\right)W_{i-1}-\left(\frac{2N_ih_k^2}{E_rI_r}+\frac{k_ih_k^4}{E_rI_r}-\beta_{lk}^4\beta_{Ai}\beta_{\rho i}\lambda^2\right)W_i$$

$$+\left(\frac{N_ih_k^2}{E_rI_r}-\frac{n_ih_k^3}{2E_rI_r}\right)W_{i+1}=0 \tag{19a}$$

$$h_k^2M_i+\beta_{Ei}\beta_{Ii}W_{i-1}-2\beta_{Ei}\beta_{Ii}W_i+\beta_{Ei}\beta_{Ii}W_{i+1}=0 \tag{19b}$$

The shear force and the rotation of the cross section are calculated using Equations (4b) and (9b), and Equations (5b), (9b), and (12b), respectively, as follows:

$$V_i = \frac{-M_{i-1} + M_{i+1}}{2h_k} \quad \text{(20a)} \qquad E_r I_r \varphi_i = \frac{-W_{i-1} + W_{i+1}}{2h_k} \quad \text{(20b)}$$

Combining Equations (2), (9b), and (20a) yields the transverse force as follows:

$$T_i = \frac{-M_{i-1} + M_{i+1}}{2h_k} + \frac{N_i h_k^2}{E_r I_r} \frac{-W_{i-1} + W_{i+2}}{2h_k^3} \tag{21}$$

2.1.3   Analysis at beam's ends and at positions of discontinuity

Positions of discontinuity are positions of concentrated mass, spring−mass system, supports, hinges, springs, abrupt change in cross section, positions where $E(x)I(x)$ is not differentiable, and change in grid spacing.

The model used in this paper (developed in Fogang [1]) consists of realizing an opening of the beam at the position of discontinuity and introducing additional points in the opening and at beam's ends. Thus, governing equations are applied at the beam's ends, as well as boundary conditions.

In case of the **W FDM** approximation, imaginary points (ia, ib, ic, and id) are introduced in the opening, and at beam's ends (-1, 0, n+2, and n+3), as represented in Figure 2. In case of the **M−W FDM** approximation, imaginary points (ia and id) are introduced in the opening, and at beam's ends (0 and n+2), as represented in Figure 2.
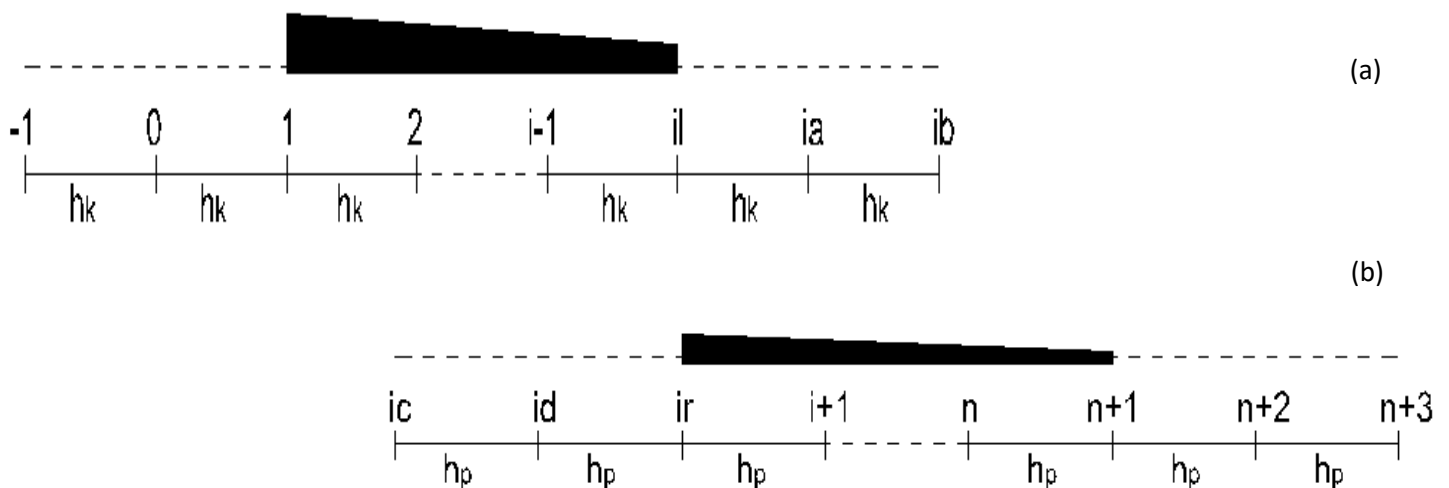
Figure 2.   Introduction of imaginary points at beam's ends and in the opening at the left side (a) and right side (b).

Thus, Equation (15) and Equations (19a-b) for W FDM and M−W FDM approximations, respectively, are applied at any point on the grid (1, 2,…i-1, il, ir, i+1…n+1 of Figure 2). The continuity equations express the continuity of the deflection and rotation of the cross section, and the equilibrium of bending moments and transverse forces. The continuity equations for deflections, rotations of cross sections, and bending moments, respectively, are defined as follows:

$$w_{il} = w_{ir} \rightarrow W_{il} = W_{ir} \tag{22a}$$

$$\varphi_{il} = \varphi_{ir} \rightarrow E_r I_r \varphi_{il} = E_r I_r \varphi_{ir} \tag{22b}$$

$$M_{il} - M_{ir} = 0 \tag{22c}$$

An adjustment of the continuity equations is made e.g. in the case of a hinge (no continuity of the rotation of the cross section; $M_{il} = M_{ir} = 0$), a support ($W_{il} = W_{ir} = 0$, no balance of transverse forces), or a spring.

In case of W FDM approximation, the bending moment and the rotation of the cross section are calculated using Equations (16a) and (16c), respectively, and in case of M–W FDM approximation the rotation of the cross section is calculated using Equation (20b). The balance of transverse forces depends on the case of discontinuity. The transverse forces T_{il} and T_{ir} in Equations (23), (25), and (27a) are calculated using Equations (17) and (21) for W FDM and M–W FDM approximations, respectively.

Effect of a concentrated force P_i: The balance of vertical forces yields

$$T_{il} - T_{ir} - P_i = 0 \tag{23}$$

Effect of a concentrated mass: The dynamic behavior of a beam carrying a concentrated mass M_p was analyzed. We set

$$M_p = m_p \times \rho_r A_r l_r \tag{24}$$

Applying Equations (12b), (14), and (24), the balance of vertical forces yields

$$T_{il} - T_{ir} - \frac{M_p \omega^2}{E_r I_r} W_{il} = 0 \rightarrow T_{il} - T_{ir} - \frac{m_p}{l_r^3} \lambda^2 W_{il} = 0 \tag{25}$$

Effect of a spring–mass system: The dynamic behavior of a beam carrying a spring–mass system was analyzed. The deflection of the mass is denoted by W_{iM}. The spring stiffness K_p is defined as follows:

$$K_p = k_p \times E_r I_r / l_r^3 \tag{26}$$

Applying Equations (12b), (14), (24), and (26), the balance of vertical forces yields

$$T_{il} - T_{ir} - \frac{M_p \omega^2}{E_r I_r} W_{iM} = 0 \rightarrow T_{il} - T_{ir} - \frac{m_p}{l_r^3} \lambda^2 W_{iM} = 0 \tag{27a}$$

$$\frac{M_p \omega^2}{E_r I_r} W_{iM} = \frac{K_p}{E_r I_r} \times (W_{iM} - W_{ir}) \rightarrow m_p \lambda^2 W_{iM} = k_p (W_{iM} - W_{ir}) \tag{27b}$$

2.2   Direct time integration method

The direct time integration method used here (developed in Fogang [1]) describes the dynamic response of a beam as a multi-degree-of-freedom system. Viscosity η and external loading p(*x,t*) are considered. The W FDM approximation is developed in this study; however the M−W FDM approximation can also be considered using appropriate formulas. The equations of dynamic equilibrium on an infinitesimal beam element are as follows:

$$E(x)I(x)\frac{\partial^4 w^*(x,t)}{\partial x^4} + 2\frac{d\left[E(x)I(x)\right]}{dx}\frac{\partial^3 w^*(x,t)}{\partial x^3} + \left[\frac{d^2\left[E(x)I(x)\right]}{dx^2} - N(x)\right]\frac{\partial^2 w^*(x,t)}{\partial x^2} +$$

$$n(x)\frac{\partial w^*(x,t)}{\partial x} + k(x)w^*(x,t) = p(x,t) - \rho(x)A(x)\frac{\partial^2 w^*(x,t)}{\partial t^2} - \eta\frac{\partial w^*(x,t)}{\partial t} \qquad (28)$$

The derivatives with respect to *x* are formulated using Equations (10a-d), while those with respect to *t* (time increment is Δt) are formulated considering a three-point stencil with Equations (29a-c):

$$\left.\frac{\partial w^*(x,t)}{\partial t}\right|_{i,t} = \frac{-w^*_{i,t-\Delta t} + w^*_{i,t+\Delta t}}{2\Delta t} \qquad \left.\frac{\partial^2 w^*(x,t)}{\partial t^2}\right|_{i,t} = \frac{w^*_{i,t-\Delta t} - 2w^*_{i,t} + w^*_{i,t+\Delta t}}{\Delta t^2} \qquad (29a)$$

At initial time t = 0, a three-point forward difference approximation is applied:

$$\left.\frac{\partial^2 w^*}{\partial t^2}\right|_{i,0} = \frac{w^*_{i,0} - 2w^*_{i,\Delta t} + w^*_{i,2\Delta t}}{\Delta t^2} \qquad \left.\frac{\partial w^*}{\partial t}\right|_{i,0} = \frac{-3w^*_{i,0} + 4w^*_{i,\Delta t} - w^*_{i,2\Delta t}}{2\Delta t} \qquad (29b)$$

At final time t = T, a three-point backward difference approximation is applied:

$$\left.\frac{\partial^2 w^*}{\partial t^2}\right|_{i,T} = \frac{w^*_{i,T-2\Delta t} - 2w^*_{i,T-\Delta t} + w^*_{i,T}}{\Delta t^2} \qquad \left.\frac{\partial w^*}{\partial t}\right|_{i,T} = \frac{w^*_{i,T-2\Delta t} - 4w^*_{i,T-\Delta t} + 3w^*_{i,T}}{2\Delta t} \qquad (29c)$$

The governing equation (Equation (28)) can be formulated with the FDM for x = i at time t. The FDM formulation of this equation is applied at any point of the beam at any time t using a seven-point stencil. Additional points are introduced to satisfy the boundary and continuity conditions. The boundary conditions are satisfied using a five-point stencil. Thus, beam deflection w*(*x,t*) can be determined with the Cartesian model represented in Figure 3. The bending moment M*(*x,t*) and transverse force T*(*x,t*) are calculated using Equations (16a) and (17), respectively.
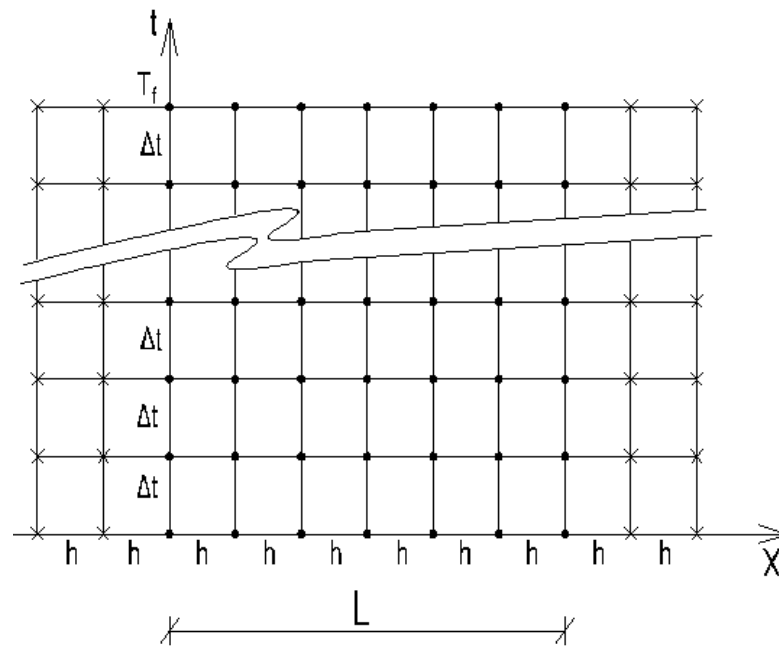
Figure 3. Model for the calculation of time-dependent vibration of axially functionally graded beams.

3   Results and discussion

3.1 Free vibration analysis of AFG tapered Euler−Bernoulli beams

We determined the vibration frequencies (coefficients λ) of AFG non-prismatic Euler−Bernoulli beams. Fixed−free, pinned− pinned, and fixed−fixed beams were considered. The geometric and material properties of the beams were represented as follows:

$$E(x)I(x) = \left[E_0 \left(1 + \frac{x}{L} \right) \right] \left[\left(1 - C_b \frac{x}{L} \right) \left(1 - C_h \frac{x}{L} \right)^3 I_0 \right],$$

$$\rho(x)A(x) = \left[\rho_0 \left(1 + \frac{x}{L} + \left(\frac{x}{L} \right)^2 \right) \right] \left[\left(1 - C_b \frac{x}{L} \right) \left(1 - C_h \frac{x}{L} \right) A_0 \right],$$

(30)

where C_b and C_h denote the width and height taper ratios, respectively, and E_0, I_0, ρ_0, and A_0 denote the elastic modulus, the moment of inertia, the beam's mass per unit volume, and the cross-sectional area, respectively, at x = 0. FDM Analysis was conducted with n = 9, 17, 33, and 49 grid points for different values of taper ratios and support conditions. Detailed results are listed in Appendix A and in the Supplementary Materials "Vibration analysis of AFG tapered Euler−Bernoulli beams W FDM approximation" and "Vibration analysis of AFG tapered Euler−Bernoulli beams M−W FDM approximation." The results of this study and those obtained by Chen [2] using the Chebyshev Collocation Method are presented in Table 1.

Table 1. Coefficients λ of natural frequencies (first mode) of AFG Euler–Bernoulli beams: Chen [2], and FDM (W FDM and M–W FDM approximations).

C_b/C_h	Chen [2]	FDM 9-pt grid		FDM 17-pt grid		FDM 33-pt grid		FDM 49-pt grid	
		W	M–W	W	M–W	W	M–W	W	M–W
Fixed–free beam									
0.0/0.0	2.4256	2.4237	2.3754	2.4250	2.4128	2.4254	2.4223	2.4255	2.4241
0.4/0.2	2.9336	2.8581	2.8946	2.9141	2.9237	2.9287	2.9311	2.9314	2.9325
0.2/0.4	2.7987	2.67272	2.7649	2.7658	2.7902	2.7904	2.7966	2.7950	2.7978
0.6/0.8	3.9232	3.3814	3.9416	3.7598	3.9278	3.8803	3.9244	3.9040	3.9237
Pinned–pinned beam									
0.0/0.0	9.0286	8.9246	8.9147	9.0024	8.9999	9.0220	9.0214	9.0256	9.0254
0.4/0.2	8.1498	8.0858	8.0449	8.1339	8.1234	8.1458	8.1432	8.1480	8.1469
0.2/0.4	7.1455	7.0821	7.0526	7.1294	7.1221	7.1415	7.1397	7.1437	7.1429
0.6/0.8	4.4263	4.0988	4.3874	4.6027	4.4136	4.4234	4.4229	4.4243	4.4247
Fixed–fixed									
0.0/0.0	20.4721	20.1752	19.2218	20.3980	20.1402	20.4550	20.3878	20.4638	20.4345
0.4/0.2	18.1286	17.9344	16.9614	18.0798	17.8178	18.1163	18.0495	18.1231	18.0933
0.2/0.4	15.8497	15.6817	14.7663	15.8031	15.5586	15.8377	15.7755	15.8444	15.8166
0.6/0.8	10.5143	7.1533	9.4032	12.4511	10.1105	10.4699	10.4002	10.4895	10.4623

The results of this study are in good agreement with those of Chen [2].

4   Conclusion

The FDM-based model developed in this paper enables, with relative easiness, vibration analysis of axially functionally graded non-prismatic Euler–Bernoulli beams. The results show that the calculations, as described in this paper, yield accurate results.

The following aspects were not addressed in this study but could be analyzed with the model in the future:

✓   Axially functionally graded Euler–Bernoulli beams resting on Pasternak foundations

✓   Elastically connected multiple-beam system

Supplementary Materials: The following files were uploaded during submission:

- "Vibration analysis of AFG tapered Euler–Bernoulli beams W FDM approximation"

- "Vibration analysis of AFG tapered Euler–Bernoulli beams M–W FDM approximation"

Funding:

Acknowledgments:

Conflicts of Interest: The author declares no conflict of interest.

Appendix A: Vibration analysis of AFG tapered Euler–Bernoulli beams

Applying Equations (11a-d), (12a), and (13a-b), the parameters $\beta_I(x)$, $\beta_A(x)$, $\beta_\rho(x)$, $\beta_E(x)$, $\beta'_{EI}(x)$, and $\beta''_{EI}(x)$ are calculated as follows:

$$\beta_I(x) = \left(1 - C_b \frac{x}{L}\right)\left(1 - C_h \frac{x}{L}\right)^3 \qquad \beta_A(x) = \left(1 - C_b \frac{x}{L}\right)\left(1 - C_h \frac{x}{L}\right)$$

$$\beta_E(x) = 1 + \frac{x}{L} \qquad\qquad \beta_\rho(x) = 1 + \frac{x}{L} + \left(\frac{x}{L}\right)^2$$

$$\beta'_{EI}(x) = \beta_{lk}\left[1 - C_b - 2C_b \frac{x}{L}\right]\left(1 - C_h \frac{x}{L}\right)^3 - 3\beta_{lk}C_h\left[1 + (1 - C_b)\frac{x}{L} - C_b\left(\frac{x}{L}\right)^2\right]\left(1 - C_h \frac{x}{L}\right)^2$$

$$\beta''_{EI}(x) = -2\beta_{lk}^2 C_b\left(1 - C_h \frac{x}{L}\right)^3 - 6\beta_{lk}^2 C_h\left[1 - C_b - 2C_b \frac{x}{L}\right]\left(1 - C_h \frac{x}{L}\right)^2 +$$

$$6\beta_{lk}^2 C_h^2\left[1 + (1 - C_b)\frac{x}{L} - C_b\left(\frac{x}{L}\right)^2\right]\left(1 - C_h \frac{x}{L}\right)$$

References

[1] Fogang, V. Euler-Bernoulli Beam Theory: First-Order Analysis, Second-Order Analysis, Stability, and Vibration Analysis Using the Finite Difference Method. Preprints 2021, 2021020559 (doi: 10.20944/preprints202102.0559.v2).

[2] Chen, W.R. Vibration Analysis of Axially Functionally Graded Tapered Euler-Bernoulli Beams Based on Chebyshev Collocation Method. International Journal of Acoustics and Vibration, Vol. 25, No. 3, 2020. https://doi.org/10.20855/ijav.2020.25.31680

[3] M. Soltani, A. Sistani, B. Asgarian. Free Vibration Analysis of Beams with Variable Flexural Rigidity Resting on one or two Parameter Elastic Foundations using Finite Difference Method. Conference Paper. The 2016 World Congress on The 2016 Structures Congress (Structures16)

[4]   K. Torabi, H. Afshari, M. Sadeghi, H. Toghian. Exact Closed-Form Solution for Vibration Analysis of Truncated Conical and Tapered Beams Carrying Multiple Concentrated Masses. Journal of Solid Mechanics Vol. 9, No. 4 (2017) pp. 760-782

[5]   P. Liu, K. Lin, H. Liu, R. Qin. Free Transverse Vibration Analysis of Axially Functionally Graded Tapered Euler-Bernoulli Beams through Spline Finite Point Method. Shock and Vibration Volume 2016, Article ID 5891030, 23 pages. http://dx.doi.org/10.1155/2016/5891030

[6]   S. Kukla, J. Rychlewska. An Approach to Free Vibration Analysis of Axially Graded Beams. Journal of Theoretical and Applied Mechanics 54, 3, pp. 859-870, Warsaw 2016. DOI: 10.15632/jtam-pl.54.3.859

[7]   Dongxing Cao, Bin Wang, Wenhua Hu and Yanhui Gao (April 22nd 2019). Free Vibration of Axially Functionally Graded Beam, Mechanics of Functionally Graded Materials and Structures, Farzad Ebrahimi, IntechOpen, DOI: 10.5772/intechopen.85835. Available from: https://www.intechopen.com/books/mechanics-of-functionally-graded-materials-and-structures/free-vibration-of-axially-functionally-graded-beam